Vesicular Microarrays

Self-Assembled Microarrays of Attoliter Molecular Vessels**

Dimitrios Stamou, Claus Duschl, Emmanuel Delamarche, and Horst Vogel**

Spatial compartmentalization is a prerequisite for the creation of living matter.[1] Without the existence of clearly defined borders,[2] differentiation and diversity at the cellular level would not be possible. Most scientific disciplines that deal with dissolved molecules are concerned with the same problem of subdividing solutions into miniaturized autonomous units, either to increase the functional complexity of a system,[3] reduce reagent consumption,[4] monitor fast chemical kinetics,[5] or even to study single molecules.[6] We describe a method that allows the parallel isolation of attoliter ($1\ aL = 10^{-18}\ L$) volumes of experimental solutions and their self-assembly into ordered arrays on surfaces with 100-nm precision. By using lipid-bilayer vesicles[1] as molecular shuttles,[7] we transported and localized molecules encapsulated in their aqueous interior or embedded in the lipid matrix. The site-selective immobilization of intact single vesicles (SVs) was mediated by patterns of receptor molecules defined by microcontact printing (μCP)[8] on glass. One-step directed self-assembly (SA)[9] produced arrays of around 10^6 volume elements per mm^2 within minutes. As shown below, this approach can create random arrays of vesicles of varied content that may serve as libraries of miniaturized experimental systems.

The strategy employed to realize arrays of surface-immobilized SVs is illustrated in Figure 1. Similar concepts have been recently applied to the immobilization of colloids[10] or vesicles[11] in regular patterns. We defined regions on the substrate that specifically bind vesicles and are surrounded by areas that prevent nonspecific attachment.

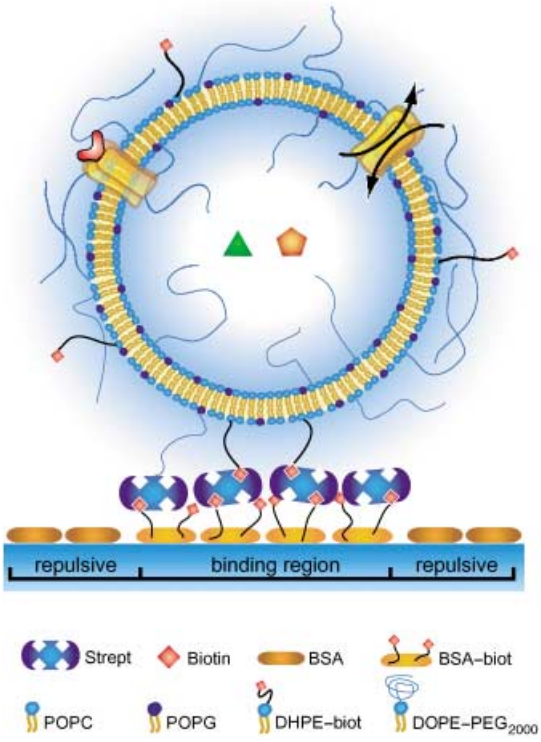

Figure 1. Strategy to self-assemble SVs on a surface with spatial control. First, biotinylated bovine serum albumin (BSA–biot) is fixed on the surface in a defined pattern by means of μCP. The nonprinted regions are passivated by adsorbtion of BSA from solution. Streptavidin (Strept) is then bound to the printed BSA–biot. Biotinylated lipids mediate the specific immobilization of vesicles. The vesicles carry charged and poly(ethylene glycol) (PEG)-derivatized lipids to prevent nonspecific interactions with the surface: 1-palmitoyl-2-oleoyl-*sn*-glycero-3-phosphocholine, POPC; 1-palmitoyl-2-oleoyl-*sn*-glycero-3-phospho-rac-(1-glycerol), POPG; *n*-((6-(biotinoyl)amino)hexanoyl)-1,2-dihexadecanoyl-*sn*-glycero-3-phosphoethanolamine, DHPE–biotin; 1,2-dioleoyl-*sn*-glycero-3-phosphoethanolamine-*n*-[methoxy (polyethylene glycol)-2000], DOPE–PEG_{2000}. The colored triangle and pentagon represent different water-soluble molecules confined in the vesicle interior.

Specific binding is mediated through the receptor–ligand pair, streptavidin–biotin.[12] Vesicles with exposed biotin ligands on their surface lock exclusively onto the parts of the substrate where the active complementary receptor was immobilized.[13] In this manner, the positioning of vesicles and their content becomes a diffusion-limited SA process guided by the patterned surface functionalization.

The properties of the vesicles can be tailored for optimum interaction with the surface by selecting an appropriate lipid composition for their bilayer. We adjusted the lipid composition to introduce two long-range repulsive forces that prevent nonspecific interactions between the vesicles and the surface. Electrostatic repulsion was controlled by setting the ratio of charged to uncharged lipids. The presence of 10% charged lipids (POPG) also increases the bending energy[14] of the lipid membrane, which prevents vesicles from deforming and fusing upon immobilization. To establish a second barrier against intimate contact between surface and vesicles, we used lipids modified with a hydrophilic polymeric chain (PEG).[15] The PEG molecules induce a force that is entropic

[*] Dr. D. Stamou, Prof. Dr. H. Vogel, Dr. C. Duschl[+]
Institut de Sciences Biomoléculaires
Ecole Polytechnique Fédérale de Lausanne, EPFL-CHB
1015 Lausanne (Switzerland)
Fax: (+41) 21-693-6190
E-mail: dimitrios.stamou@epfl.ch
horst.vogel@epfl.ch
Dr. E. Delamarche
IBM Research
Zurich Research Laboratory
8803 Rüschlikon (Switzerland)
[+] Present address: Fraunhofer Institute
Biomedical Technology (AMBT)
Invalidenstrasse 42, 10115 Berlin (Germany)

[**] We thank A. Brecht and C. Bieri for critically reading the manuscript, and A. Bietsch and B. Michel for the high-resolution μCP stamps. This work was in part funded by the TOP NANO 21 program and the IHP/Networks Programme of the European Community (Project HPRN-CT-2000-00159).

Supporting information for this article is available on the WWW under http://www.angewandte.org or from the author.

  DOI: 10.1002/ange.200351866

in nature and independent of the immobilization conditions (pH, ionic strength) that affect electrostatic-based repulsion. To maintain the membrane in a fluid state and avoid leakage, POPC was chosen as the main lipid constituent, which ensured an ordered-to-fluid phase transition far below room temperature. A balance of contributions from the three most important interactions, that is, the receptor–ligand binding, the electrostatic repulsion, and the entropic repulsion, was crucial to achieving selective deposition of intact vesicles.

We chose the dimensions of the vesicles and the resolution of the patterning method to be complementary to the probe volume of fluorescence-based detection techniques. Most of the vesicles used in this work were prepared by extrusion, with an average diameter of 100 nm.[16] The surface onto which the vesicles are immobilized was structured by μCP, a versatile technique for patterning surfaces with a variety of biomolecules[17] with a resolution of less than 100 nm.[18] In this patterning step, we directly defined both the geometry and the resolution of the subsequent vesicle assembly.

One strategy to immobilize small numbers of vesicles onto predefined areas of a surface is to reduce the number of vesicles available for binding per printed area. This reduction is readily accomplished in the SA step by reducing the vesicle concentration. The fluorescence image in Figure 2a shows vesicles with an average diameter of 100 nm immobilized on an array composed of 2-μm-wide dots separated by 8 μm. The vesicles are localized within ± 1 μm of the center of the printed areas. Vesicles did not bind to surfaces preincubated with biotin (results not shown), which emphasizes the specificity of this immobilization procedure and indicates the successful suppression of nonspecific interactions by this approach. The occupation of potential binding regions was on the order of 80%. The mean number of vesicles per dot is estimated to be 1.3 (all resolved features were assumed to be SVs because their solution density was too low). To verify that vesicles neither leaked nor fused with the surface upon immobilization, we loaded them with the water-soluble dye carboxyfluorescein. Figure 2b shows the simultaneously recorded fluorescence emmision originating from the membrane and from the interior of the vesicles and the co-localization of the two signals. CF was retained for periods of several days, which proves that the immobilized vesicles had an ability to confine molecules that is comparable to that of vesicles in suspension. As long as equiosmolar solutions were used, immobilized vesicles were stable against washes/buffer exchange. The absence of nonspecific deposition of vesicles together with the precise localization of the immobilized vesicles create the contrast that is key for proceeding to the immobilization of single vesicles.

Extension of the technique from statistical placement of small numbers of vesicles on predefined areas to SV positioning required reduction of the pattern size to the dimensions of the vesicles.[10] We functionalized glass by using high-resolution μCP stamps that had various features with sizes as small as 60 nm.[18] The simultaneous presence of different patterns on the surface allowed us to screen in one step for the geometries and sizes that were appropriate for immobilization of a single vesicle on a printed feature. The highest occupation of printed sites by SVs (80%) was obtained for

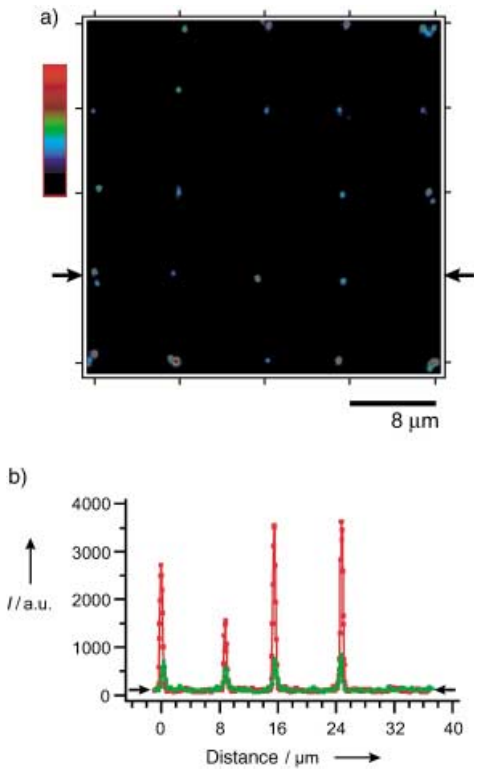

Figure 2. Confocal fluorescence microscopy characterization of groups of vesicles arrayed on a glass surface (LSM 510, Zeiss). Binding sites were 2 μm in diameter and situated on an 8-μm quadratic lattice. Vesicles were labeled with 1% rhodamine–lipid in the bilayer and loaded with d-sorbitol (200 mM) and carboxyfluorescein (CF; 100 μM, approximately 30 CF molecules per 100-nm vesicle). a) Fluorescence from the lipid bilayer indicates the position of the vesicles. b) Line trace from the image in (a) showing the rhodamine signal (red) and the simultaneously acquired fluorescence signal of CF (green). The vesicles are positioned site-specifically on the surface and remain intact, as indicated by their retention of CF.

'linelets' with dimensions of 100×400 nm^2 spaced 800 nm apart (Figure 3a). Vacancies (for example, first row, positions 2 and 5 in Figure 3a) are due to patterning defects (incomplete stamping) and size-related binding constraints (for example, number of receptors available). Decreasing the size of the patterns lowered the occupation percentage, whereas increasing it resulted in multiple occupation (results not shown). Vesicles are localized on the linelets to within ± 50 nm in the vertical and ± 200 nm in the horizontal direction. The vesicles are kept at an average separation of 800 nm, which is twice their resolution-limited diameter. The different intensities observed probably originate from differences in size and, therefore, different numbers of fluorophores per vesicle. Incubation times to self-assemble vesicles onto printed sites were 5–10 min for vesicle concentrations of 3 nM.

In addition we incubated the linelet patterns with a mixture of two vesicle populations, each tagged with a different fluorophore (Figure 3b). The occupation of one site by multiple vesicles would result in the co-localization of the two fluorescence signals. No co-localization was observed, which proves that each occupied site of the pattern contains only one vesicle. The size of the arrays we fabricated was $0.4 \times$

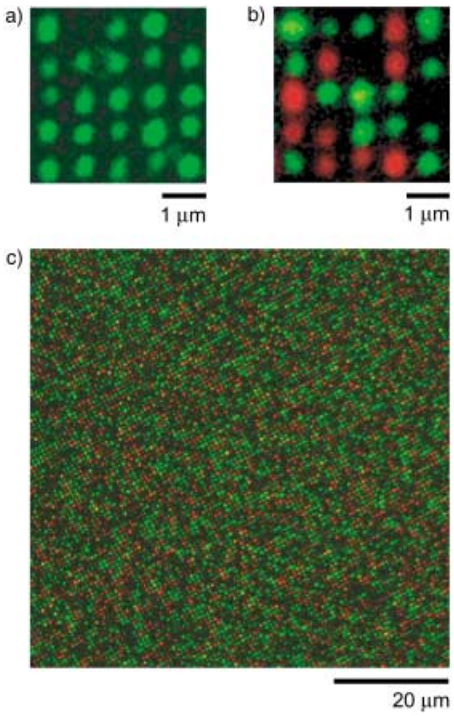

Figure 3. High-density arrays of SVs immobilized on 100×400-nm^2 binding sites, separated by 800 nm. The confocal fluorescence images show a) an array of one type of vesicles labeled with oregon488–lipid, and b) the same patterns incubated with a mixture of two differently labeled vesicle populations (red: rhodamine; green: oregon488). Overlay of the two signals shows no co-localization of fluorescence, which proves that only one vesicle is immobilized per binding site. c) Directed SA permits the construction of complex high-density SV arrays over large areas.

0.4 mm^2 and this size can be extended into the centimeter range. The fluorescence image in Figure 3c shows a small part of a mixed array with an SV density of about 10^6 mm^{-2}. All SVs in the image are placed in an ordered fashion on the surface, which renders their localization simple. The positioning of different SVs on the array is random, but various encoding schemes (such as oligonucleotide tagging) can be employed to ascertain the identity of each SV, even in the case of complex mixtures.[19]

To assess the stability of the controlled environment of molecules confined inside immobilized vesicles, we investigated the permeability of the lipid bilayer. Low passive influx/efflux of ions into/out of vesicles is a prerequisite for keeping the pH value or ionic composition of an SV stable and the function of a protein or the reactivity of solutes inside an SV reliable. The experiments whose results are reported in Figure 4 take advantage of the pH sensitivity of CF to monitor the pH value inside SVs 0.5–1 μm in diameter, immobilized on 10-μm-wide stripes. The vesicles were prepared with a pH value of around 5.5 and were immobilized in a buffer of pH 7.4. After immobilization, the pH value of the vesicles shifted to about 6.2, where it remained stable because of the established diffusion potential (Figure 4, Experiment A). The SVs proved capable of maintaining pH gradients of more than one unit over the course of several hours as a result of the low counterion exchange rate.

In a subsequent step, we addressed the interior of these tightly sealed containers and initiated a simple chemical reaction. We triggered the deprotonation of CF inside the SVs by treatment with an ion-channel-forming peptide (gramicidin A). Gramicidin forms cation-selective channels in lipid membranes. Upon incorporation into a bilayer, the channels allow Na^+ ions to diffuse down their concentration gradient, in this case into the vesicle. The sodium influx induces a pH increase (proton efflux) so as to maintain electroneutrality. In Experiment B shown in Figure 4, we monitored individual vesicles over time and recorded how the fluorophores trapped in their interior responded to the gramicidin stimulus. As a result of the high single-channel conductance of gramicidin

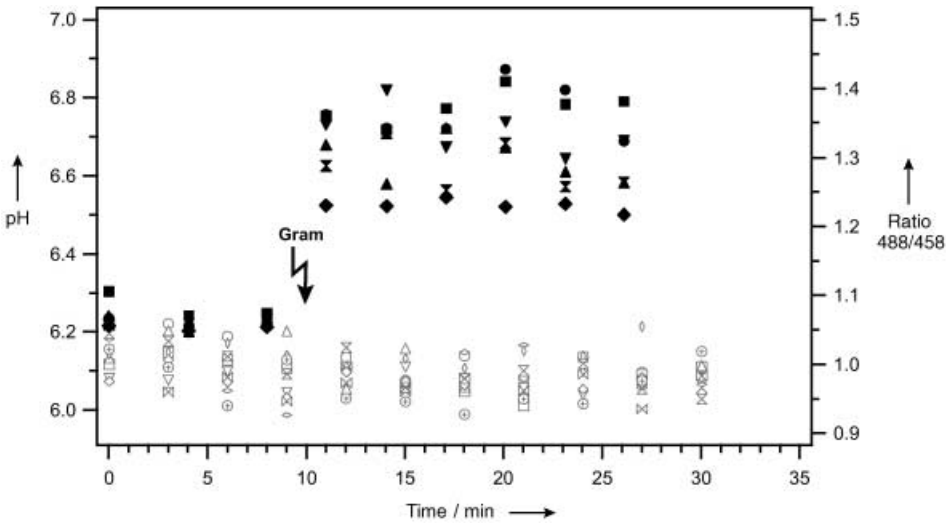

Figure 4. The internal pH value of SVs monitored over time. Vesicles were loaded with CF (100 μM). The pH value was inferred from the excitation ratio 488/458 nm of the dye, at an emission bandwidth of 505–550 nm (see the Supporting Information). Experiment A (open symbols) monitored the stable pH value of SVs after their immobilization. In Experiment B (solid black symbols), we triggered a chemical reaction (deprotonation of CF) in the interior of the SVs in a second sample by the addition of gramicidin (Gram; 10 nM). In both experiments, we selected vesicles 0.5–1 μm in diameter to ensure a sufficient number of fluorophores were present. For clarity, the results of Experiment A are shifted vertically by −0.1.

(~40 pS), equilibrium was reached milliseconds after the first channel opened,[20] much faster than the time resolution of the results shown in Figure 4 (see also the Supporting Information). Ion channels with smaller conductivities (for example, the 5-HT_{3A} receptor[21]) would need seconds or minutes to establish equilibrium and would therefore potentially allow real-time monitoring of channel activity.[22] This experiment illustrates how the selective permeability properties of membrane-associated transporters or channels can be employed to perform chemistry inside individually addressed nanocontainers.

Hierarchical SA is an emerging approach to the fabrication of functional nanometer-scale architectures.[9] In this work, we combined SA principles and receptor–ligand interactions first to define attoliter autonomous experimental volumes, and then to order them on a surface. Incorporation of multifunctional recognition elements, such as oligonucleotides, would further increase the complexity of the assembled structures.[23] The lipid-bilayer vesicles we used as molecular vessels are arrayed at high densities (every 800 nm, $\sim 10^6\ mm^{-2}$). Nevertheless, each one maintains its cargo dissolved in a protective environment[24] of defined chemical composition (pH, ionic strength, etc.) and at the same time localizes its position with 100-nm precision. Such ultrasmall-volume libraries allow simultaneous screening[6] of (bio)-chemical properties, molecular function, or confined chemical reactions over millions of samples, while consuming total reagent volumes of a few picoliters. A natural extension of this work is the use of vesicles produced directly from cells to form arrays.[25] To array native vesicles individually, the employment of a more versatile surface modification[26] might be crucial since their properties are not so easily controlled as those of synthetic vesicles. Native vesicles are of primary importance as they can carry receptor proteins expressed in cell membranes and/or signal transduction machinery from the cytosol. In array format, such vesicles may thus be used to screen binding of pharmaceutical compounds (drug candidates) or the functional responses induced by such binding.

Experimental Section

Vesicle production: A dried lipid film was rehydrated overnight in d-sorbitol (200 mM). A vesicle cloud was then harvested (ca. 1 $mg\,mL^{-1}$), freeze-thawed, and extruded through 100-nm filter pores (typical vesicle diameters were 100 ± 40 nm). The vesicles used for the experiments in Figure 4 were passed once through a 1-μm pore-size filter after harvesting to create a sharp upper cut-off in their size distribution. Before incubation with the microarray surface, vesicles were diluted (1:10) in the immobilization buffer (80 mM NaCl and 10 mM $NaHPO_4$ at pH 7.4). All experiments presented herein used vesicles composed of POPC (88%), POPG (10%), DHPE–biot (2%), and DOPE–PEG_{2000} (0.3%). We used two fluorescently labeled lipids: *n*-(6- tetramethylrhodaminethiocarbamoyl)-1,2- dihexadecanoyl-*sn*-glycero-3- phosphoethanolamine and Oregon green 488–1,2-dihexadecanoyl-*sn*-glycero-3-phosphoethanolamine.

Patterned surface functionalization: Poly(dimethylsiloxane) stamps for μCP were inked with BSA–biot ($0.1\ mg\,mL^{-1}$). After washing the stamps with phosphate-buffered saline and removing residual buffer under an N_2 stream, we printed BSA–biot onto a clean glass substrate, which was subsequently passivated with BSA ($0.5\ mg\,mL^{-1}$). The patterned substrate was then functionalized by incubation with streptavidin ($0.025\ mg\,mL^{-1}$) for 10 min. The final streptavidin surface density was approximately 10% of a complete monolayer.

Received: May 12, 2003 [Z51866]
Published Online: November 5, 2003

Keywords: liposomes · microarrays · nanostructures · self-assembly · vesicles

[1] R. Lipowsky, E. Sackmann, *Structure and Dynamics of Membranes. From Cells to Vesicles*, Elsevier Science, Amsterdam, **1995**.
[2] R. B. Gennis, *Biomembranes. Molecular Structure and Function*, 1st ed., Springer, New York, NY, **1989**.
[3] A. Bernard, B. Michel, E. Delamarche, *Anal. Chem.* **2001**, *73*, 8.
[4] A. v. d. Berg, W. Olthouis, P. Bergveld, *Micro Total Analysis Systems 2000*, Kluwer Academic, Dordrecht, **2000**.
[5] K. Jensen, *Nature* **1998**, *393*, 735.
[6] M. J. Levene, J. Korlach, S. W. Turner, M. Foquet, H. G. Craighead, W. W. Webb, *Science* **2003**, *299*, 682.
[7] D. T. Chiu, C. F. Wilson, F. Ryttsen, A. Stromberg, C. Farre, A. Karlsson, S. Nordholm, A. Gaggar, B. P. Modi, A. Moscho, R. A. Garzalopez, O. Orwar, R. N. Zare, *Science* **1999**, *283*, 1892.
[8] B. Michel, A. Bernard, A. Bietsch, E. Delamarche, M. Geissler, D. Juncker, H. Kind, J. P. Renault, H. Rothuizen, H. Schmid, P. Schmidt-Winkel, R. Stutz, H. Wolf, *IBM J. Res. Dev.* **2001**, *45*, 697; Y. Xia, G. M. Whitesides, *Angew. Chem.* **1998**, *110*, 568; *Angew. Chem. Int. Ed.* **1998**, *37*, 551.
[9] G. M. Whitesides, B. Grzybowski, *Science* **2002**, *295*, 2418.
[10] Y. D. Yin, Y. Lu, B. Gates, Y. N. Xia, *J. Am. Chem. Soc.* **2001**, *123*, 8718.
[11] S. Svedhem, I. Pfeiffer, C. Larsson, C. Wingren, C. Borrebaeck, F. Hook, *ChemBioChem* **2003**, *4*, 339; R. Michel, I. Reviakine, D. Sutherland, C. Fokas, G. Csucs, G. Danuser, N. D. Spencer, M. Textor, *Langmuir* **2002**, *18*, 8580.
[12] S. A. Walker, M. T. Kennedy, J. A. Zasadzinski, *Nature* **1997**, *387*, 61.
[13] A. Albersdorfer, T. Feder, E. Sackmann, *Biophys. J.* **1997**, *73*, 245.
[14] R. Lipowsky, *Nature* **1991**, *349*, 475.
[15] D. Kroger, F. Hucho, H. Vogel, *Anal. Chem.* **1999**, *71*, 3157.
[16] B. J. Frisken, C. Asman, P. J. Patty, *Langmuir* **2000**, *16*, 928.
[17] C. Bieri, O. P. Ernst, S. Heyse, K. P. Hofmann, H. Vogel, *Nat. Biotechnol.* **1999**, *17*, 1105.
[18] J. P. Renault, A. Bernard, A. Bietsch, B. Michel, H. R. Bosshard, E. Delamarche, M. Kreiter, B. Hecht, U. P. Wild, *J. Phys. Chem. B* **2003**, *107*, 703.
[19] D. R. Walt, *Science* **2000**, *287*, 451.
[20] C. M. Biegel, J. M. Gould, *Biochemistry* **1981**, *20*, 3474.
[21] S. P. Kelley, J. I. Dunlop, E. F. Kirkness, J. J. Lambert, J. A. Peters, *Nature* **2003**, *424*, 321.
[22] M. Tschodrich-Rotter, U. Kubitscheck, G. Ugochukwu, J. T. Buckley, R. Peters, *Biophys. J.* **1996**, *70*, 723.
[23] L. M. Demers, D. S. Ginger, S. J. Park, Z. Li, S. W. Chung, C. A. Mirkin, *Science* **2002**, *296*, 1836.
[24] E. Rhoades, E. Gussakovsky, G. Haran, *Proc. Natl. Acad. Sci. USA* **2003**, *100*, 3197.
[25] D. T. Chiu, S. J. Lillard, R. H. Scheller, R. N. Zare, S. E. Rodriguez-Cruz, E. R. Williams, O. Orwar, M. Sandberg, J. A. Lundqvist, *Science* **1998**, *279*, 1190.
[26] R. Michel, J. W. Lussi, G. Csucs, I. Reviakine, G. Danuser, B. Ketterer, J. A. Hubbell, M. Textor, N. D. Spencer, *Langmuir* **2002**, *18*, 3281.

